AC losses in HTS coils for high-frequency and non-sinusoidal currents

Citation for published version (APA):
de Bruyn, B. J. H., Jansen, J. W., & Lomonova, E. A. (2017). AC losses in HTS coils for high-frequency and non-sinusoidal currents. *Superconductor Science and Technology*, *30*(9), Article 095006. https://doi.org/10.1088/1361-6668/aa7c74

DOI:
10.1088/1361-6668/aa7c74

Document status and date:
Published: 01/09/2017

Document Version:
Accepted manuscript including changes made at the peer-review stage

Please check the document version of this publication:

• A submitted manuscript is the version of the article upon submission and before peer-review. There can be important differences between the submitted version and the official published version of record. People interested in the research are advised to contact the author for the final version of the publication, or visit the DOI to the publisher's website.
• The final author version and the galley proof are versions of the publication after peer review.
• The final published version features the final layout of the paper including the volume, issue and page numbers.

Link to publication

General rights
Copyright and moral rights for the publications made accessible in the public portal are retained by the authors and/or other copyright owners and it is a condition of accessing publications that users recognise and abide by the legal requirements associated with these rights.

- Users may download and print one copy of any publication from the public portal for the purpose of private study or research.
- You may not further distribute the material or use it for any profit-making activity or commercial gain
- You may freely distribute the URL identifying the publication in the public portal.

If the publication is distributed under the terms of Article 25fa of the Dutch Copyright Act, indicated by the "Taverne" license above, please follow below link for the End User Agreement:

www.tue.nl/taverne

Take down policy
If you believe that this document breaches copyright please contact us at:

openaccess@tue.nl

providing details and we will investigate your claim.

Download date: 08. Jul. 2024

AC Losses in HTS Coils for High-Frequency and Non-Sinusoidal Currents

B.J.H. de Bruyn, J.W. Jansen, and E.A. Lomonova
Eindhoven University of Technology, Electromechanics and Power Electronics Group, Department of Electrical Engineering,
PO Box 513, 5600 MB, Eindhoven, The Netherlands

***Abstract*—AC losses in racetrack coils that are wound of YBCO tapes are measured for sinusoidal and non-sinusoidal transport currents with fundamental frequencies up to 1 kHz. An electrical method to measure losses for non-sinusoidal currents is developed for this purpose. The measured losses are compared to the losses calculated by 2D finite element models with power-law material models. The frequency and waveform-dependency of the measured losses are shown, and compared to the results of the models over a wide range of frequencies and waveforms. Finally, it is shown that the finite element models can accurately predict AC losses resulting from non-sinusoidal transport currents as are present in highly dynamic motors with AC armature coils.**

***Index Terms*—Superconducting coils, type II Superconductors, AC losses, loss measurement, finite element analysis**

I. Introduction

CURRENTLY, the main applications for high-temperature superconducting (HTS) tapes are DC-field generation and large power conversion systems. These either operate with DC current or sinusoidal currents at low (<100 Hz) frequencies. For this reason, most investigations on AC losses in superconducting coils have focussed on sinusoidal currents with a frequency around 50 Hz [1]–[3]. Measurements of AC losses have been reported for sinusoidal currents with frequencies up to 800 Hz in coils [4]–[6] and up to 3800 Hz for tapes [7]. In these measurements the losses per cycle increase slightly with frequency, due to thermally activated flux creep and eddy current losses in the copper sheats. Some measurements have been performed for low-frequency non-sinusoidal currents [8], and it was shown that losses related to the addition of a third harmonic can be accurately predicted. To open the way for new superconducting power applications, measurement methods and validated loss models for arbitrary non-sinusoidal and high-frequency currents are required. Examples of these applications are higher harmonics in power applications and non-sinusoidal currents in highly dynamic superconducting motors [9].

The three main principles of AC loss measurement for superconducting coils are calorimetric, magnetic, and electrical measurement methods. Calorimetric measurement methods measure the local losses by the local temperature increase [10], or the global losses by the boil-off of the liquid coolant. These methods allow for any waveform of the current [11], [12], but only work at the boiling temperature of the liquid coolant. Magnetic measurement methods measure hysteresis in the magnetic field, and require a pickup coil enclosing the coil under test [13], [14]. These methods require calibration of the ratio between the hysteresis loop area and losses in the coil. Finally, electrical measurement methods exist using lock-in amplifiers to measure the phase difference between the first harmonic of the coil current and voltage. These methods are only able to measure the losses related to the first harmonic of the applied currents, and are therefore only valid for sinusoidal currents.

TABLE I
Parameters of wound coils.

Coil #	Tape ID	Tape critical current	# turns
1	M3-1036-2 MS	111	28
2	M4-153-2 FS	124	28

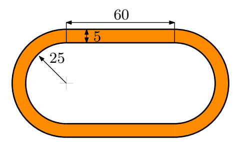

Fig. 1. Dimensions of the manufactured coils in mm.

In this paper, an electrical measurement method is developed which is able to measure losses for high-frequency and non-sinusoidal currents. The method is based on direct measurement of the coil voltage and current, and is calibration-free, temperature independent and fast. An analysis of the main error components in the proposed measurement method is given. The AC losses are measured for sinusoidal currents up to 1 kHz, and for non-sinusoidal currents with various waveforms including a waveform typical for high-dynamic motor applications. The measurements are compared to finite elements models and analytical models. Finally, conclusions are given on the modeling of high-frequency behavior of HTS superconducting coils.

II. Methods

A. Manufacturing of superconducting coils

Two racetrack coils of 4 mm wide YBCO tape produced by Superpower were wound on electrically non-conductive G11 coil formers. The coils were wound with the superconducting layer on the inside of the coil, with respect to the non-magnetic substrate. A 5 mm wide polyimide adhesive tape was applied to the tapes before winding, for electrical insulation. The parameters of the coils and tapes, are shown in Table I. The dimensions of the coils in mm are shown in Fig. 1. The inductance of the coils was measured to be around 160 μH. The exponential $I-V$ characteristics of a section of tape were

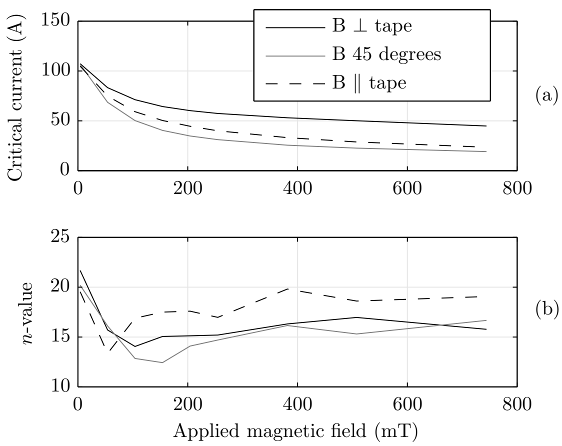

Fig. 2. Measured parameters of $I-V$ curves of coil 1 as function of applied magnetic field (a) critical current (b) values of the exponent n.

measured for a range of applied magnetic flux densities and angles with respect to the tape. The critical current I_C and n-value were determined by a least-squares fit of the function

$$V = E_C \left(\frac{I}{I_C} \right)^n \tag{1}$$

to the data, with a critical current criterion of $E_C = 1$ μV/cm. These parameters are shown in Fig. 2. The critical current for magnetic field applied at an angle of 45 degrees to the tape is the lowest. Also, the data show that the critical current density for magnetic field applied perpendicular to the tape is higher than the critical current density for magnetic field applied parallel to the tape. This is remarkable, since most publications show that the decrease in critical current is strongest for magnetic field applied perpendicular to the tape. However, measurement data of various superconducting tapes, given in [15] shows that at temperatures of 77 K, and for applied magnetic fields lower than 1 T, this is not necessarily true. The results for coil 2 were similar, and the field-free critical current of this coil was equal to 125 A. The measured dependency of the critical current on the applied magnetic field is included in the models.

B. Principle of measurement

Electrical measurement methods generally only measure losses for purely sinusoidal applied currents. The losses are determined from the phase difference between the current and voltage of a coil, measured by a lock-in amplifier. Periodical currents i and voltages v can generally be written as

$$i = i_0 + \sum_{n=1}^{\infty} a_n \sin(n\omega t + \alpha_n), \tag{2}$$

$$v = v_0 + \sum_{n=1}^{\infty} b_n \cos(n\omega t + \beta_n), \tag{3}$$

where a_n, b_n, α_n, and β_n are constants. For purely sinusoidal currents, the average power losses are then given by

$$P = i_0 v_0 + \frac{1}{2} a_1 b_1 \sin(\alpha_1 - \beta_1). \tag{4}$$

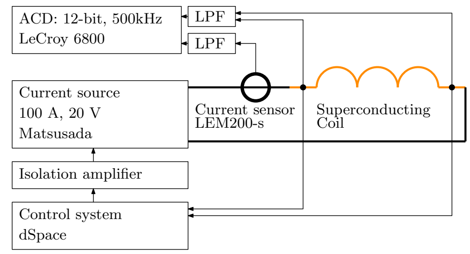

Fig. 3. Schematic representation of the measurement instrument.

Therefore, in this case, losses can be determined from the phase difference between the first harmonics of voltage and current, even if higher harmonics in the voltage exist due to the nonlinearity of the superconducting materials.

However, if the applied current is non-sinusoidal, the higher harmonics of the current also contribute to the losses. Because the superconducting material is highly nonlinear, the AC losses are not necessarily equal to a linear contribution of the losses resulting from the separate harmonics of the current. Therefore, a direct electrical AC loss method, which also works for non-sinusoidal current waveforms was implemented. The method is based on direct measurement of voltage and current over the superconducting coil or tape. The average power P delivered to the coil is calculated as

$$P = \frac{1}{t_m} \int_{t=t_0}^{t=t_0+t_m} iv \, dt = P_{stored} + P_{loss}. \tag{5}$$

The power consists of the time-averaged stored power P_{stored} and the average losses P_{loss}. For a signal with period T, the measurement time t_m is chosen as an integer multiple of T. In this way, the stored power is equal to zero, and the average power is equal to the average losses.

C. Measurement instrument

Figure 3 shows an overview of the measurement instrument. Current waveforms are generated by a dSpace control system, coupled to a current source by an isolation amplifier. The current source is a Matsusada 4-quadrant amplifier, with a current bandwidth of 20 kHz, peak output current of ±100 A, and peak output voltage of ±20 A. The transport current is measured by a LEM200-s ultrastab current transducer, with a 500 kHz bandwidth. The coil voltage and the current signal are recorded on a LeCroy HDO4024 12-bit digital oscilloscope. Two analog 20 kHz first-order analog low-pass filters are used on the input of the oscilloscope, which reduce aliasing errors in the measured signals. Both voltage and current signals are filtered, and the component values of the filters are matched, such that both signals have an equal phase shift. By simulations of the measurement signals, a sampling frequency of 500 kHz is chosen such that the measurement error resulting from aliasing is sufficiently small.

The two main error sources in the losses measured by the instrument are voltage noise and time delay between the measured voltage and current signals. For samples having a

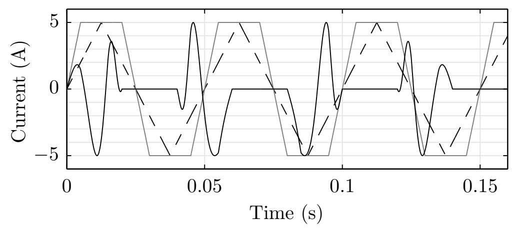

Fig. 4. Current waveforms of triangular, trapezoidal, and high-dynamic currents used in loss measurements.

standard deviation of σ, the standard deviation of the mean of N samples, $\bar{\sigma}$, is given by

$$\bar{\sigma} = \frac{\sigma}{\sqrt{N}}. \tag{6}$$

Therefore, the standard deviation in the measured losses σ_l, for a given standard deviation in the voltage noise σ_v, is approximately given by

$$\sigma_l = \frac{I_{rms}\sigma_v}{\sqrt{N}}, \tag{7}$$

where I_{rms} is the rms value of the applied current. During the measurements, the voltage and current are sampled for 2 seconds at 500 kHz, and the voltage noise level is approximately 30 mV.

A time delay Δt between the measured voltage and current signals, for sinusoidal current with frequency f, gives an offset in the measured losses P_{offset} of

$$P_{offset} = L_{coil} I_{pk}^2 \pi f \sin(2\pi f \Delta t), \tag{8}$$

where L_{coil} is the self-inductance of the coil. This error increases with frequency, and the error relative to the actual AC losses are highest for high-frequency currents at low amplitude. A time delay of 0.45 μs was determined by calibration and is corrected in the post-processing.

D. Measurement procedure

Measurements are performed at liquid nitrogen temperature (77 K). The AC losses are measured for transport currents at different frequencies, with various peak values, and with various waveforms. These waveforms are sinusoidal, triangular, trapezoidal, and a waveform as present in a highly dynamic motor applications where the superconducting coils carry AC currents. The waveforms are shown for a frequency of 20 Hz in Fig. 4. The length of the flat tops of the trapezoidal current are equal to 3/10 of the period of the signal. For the motor current, which has a repetition time of 160 ms, only the amplitude of the applied current is varied. The amplitude of the applied currents is limited by the maximum inductive voltage over the coils, which depends on the waveform and frequency.

III. Modeling of AC losses

The AC losses in the racetrack coils are modeled by a 2D finite element model, which models an infinitely long stack of 28 superconducting tapes. The transient model, based on the H-formulation [16], is implemented in Comsol [17]. The AC losses in the model are calculated for two full periods of the applied current, and the mean losses in the second full period are compared to the measured losses. In the model, only the superconducting layers are modeled. The resistivity of the superconducting tape, ρ, is modeled according to the power-law model as

$$\rho = \frac{E_c}{J_c}\left(\frac{J}{J_c}\right)^{n-1}, \tag{9}$$

where J is the current density in the superconducting material, and J_c is the critical current density. The critical current density is determined from the measured critical current as

$$J_c = \frac{I_c}{A}, \tag{10}$$

where A is the cross-section of the superconducting layer. Hereby it is assumed that the superconducting material is homogeneous. The self-consistency of the modeling and measurement of the $I-V$ curves is checked by modeling the DC critical current measurement of a single strip. It was found that the simulated $I-V$ curve agrees with the modeled material parameters within 0.5%.

In the finite element implementation, the current density is homogeneous in each mesh element. If the mesh is too coarse, the critical current density is not reached even if the total current of one tape flows through one mesh element. In that case, the losses will be underestimated by the model. Therefore, the number of mesh elements in the height of the tape, m, is chosen to be at least

$$m = \frac{I_c}{4I_{pk}}, \tag{11}$$

where I_c is the critical current of a single tape, and I_{pk} is the peak value of the current applied to the tape.

The AC losses are additionally estimated by an analytic equation, which assumes the critical state model. This model does not take into account the field-dependency of the critical current, and is equivalent to the power-law model for $n = \infty$. For a stack of an infinite number of superconducting tapes where a transport current is applied varying monotonously from $-I_0$ to $+I_0$ and back, the AC losses in Joule per meter of tape per cycle of the applied current, are given by [18] as

$$Q = Q_c i_0^2 \int_{s=0}^{s=1} (1-2s)\ln\left[\frac{\cosh^2(\pi a/L_y)}{\cosh^2(\pi i_0 s a/L_y)}\right] ds, \tag{12}$$

where $Q_c = \mu_0 I_c^2/\pi$, $I_0 = I_{pk}/I_c$, a is the half-width of the tape, and L_y is the spacing between the tapes. For this model the losses per cycle are independent of frequency and are equal for sinusoidal, triangular and trapezoidal waveforms.

IV. Results and analysis

A. Results models

The losses per cycle of the current calculated by the finite element models depend on the n-value, the frequency and the waveform of the currents. The calculated losses in coil 1 as function of the n-value, for currents with a peak value of 40 A and a frequency of 50 Hz and 1 kHz are shown in Fig. 5. The modeled losses are lower than those given by (12), because an

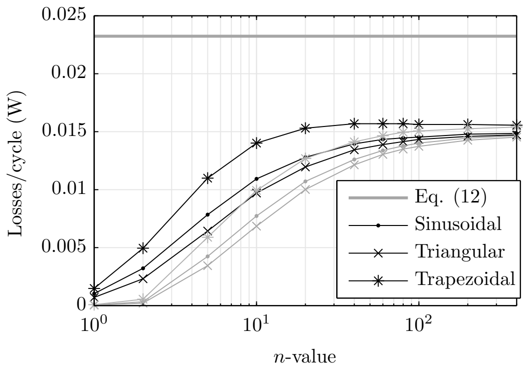

Fig. 5. Modeled AC losses per cycle as function of the n-value, for 50 Hz (black lines) and 1 kHz (gray lines) currents with various waveforms with a peak value of 40 A in coil 1.

infinite stack of tapes is assumed there. For all waveforms, the calculated losses per cycle at 1 kHz are lower than those at 50 Hz. Both the frequency-dependency and the dependency of the losses on the waveforms decrease towards higher n-values. This indicates that the model contains mixed hysteretic and resistive behavior. For an n-value equal to 1, the material is modeled as a linear resistivity. In this case, the losses are a combination of resistive losses related to the rms current and losses related to induced currents which depend on the frequency. For an n-value close to infinity, the behavior of the losses is purely hysteretic. In this case, the losses per cycle are independent of frequency. For the n-values typical for HTS tapes, between 10 and 30, the modeled behavior is weakly frequency dependent [19], [20]. Finally, the model predicts that, for equal peak values of the currents, the AC losses for trapezoidal currents are higher than those for sinusoidal currents, and for triangular currents the losses are lower than those for sinusoidal currents. This is related to the resistive contribution to the losses, the rms value of the trapezoidal currents are 21% higher than that of sinusoidal currents and the rms value of the triangular currents are 18% lower than that of sinusoidal currents. In all models, the n-value was equal to 20, corresponding to the measured value of the tapes for low applied magnetic fields.

B. Results measurements and models

The AC losses measured for coil 1 and coil 2, for sinusoidal currents at different frequencies and amplitudes, are shown in Fig. 6. The mean difference between the measured values of the coils is 1%, while the mean of the absolute value of the difference is equal to 15%. These results show that the loss measurements are repeatable, even for coils wound from tapes with different parameters. Since the measurements are not sensitive to small changes in tape parameters, it is expected that the losses can be modeled with similar correspondence. In the remainder of the paper, only measurement and modeling results of coil 1 are shown.

The simulated and measured losses per cycle of sinusoidal current are shown for different peak currents in Fig. 7. The losses per cycle as function of frequency in the measurements

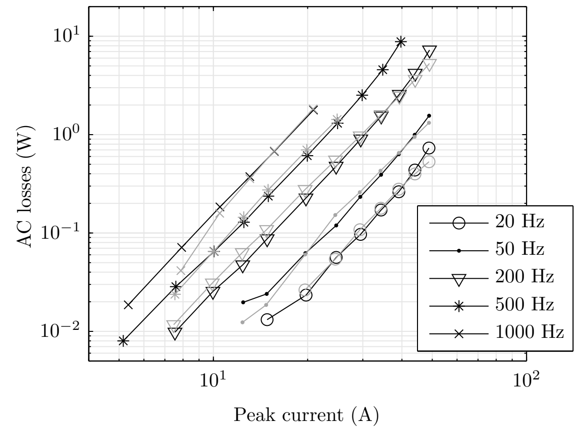

Fig. 6. Measured AC losses for sinusoidal currents in coil 1 (black lines) and coil 2 (gray lines).

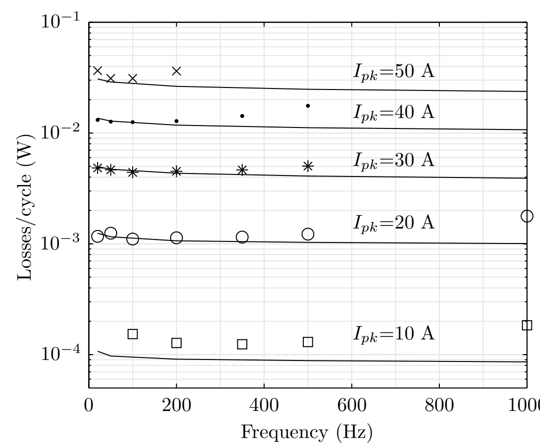

Fig. 7. Measured (symbols) and modeled (lines) AC losses per cycle of sinusoidal current for different peak values of the current.

follow the decreasing trend in the simulations for low frequencies. The frequency at which the minimal losses per cycle are measured depends on the peak value of the current. For peak currents of 50 A the losses per cycle are minimal at 100 Hz, while for peak currents of 10 A the losses per cycle are minimal at 350 Hz. At higher frequencies, the measured losses increase with frequency, while the simulated losses decrease with frequency over the full range. The increase in measured losses at higher frequencies and peak amplitudes is related to eddy current losses in the non-superconducting layers [21] and to the slow thermal diffusion and increase of the temperature of the superconducting coil at high loss values [22].

The dependency of the measured AC losses on the different waveforms is shown in Fig. 8. The figure shows that the AC losses for trapezoidal waveforms are higher than those for sinusoidal waveforms, and the AC losses for triangular waveforms are lower than those for sinusoidal waveforms, as is predicted by the finite element models.

The measured and modeled losses for sinusoidal, triangular, and trapezoidal current waveforms at 20 Hz and 200 Hz are shown in Fig. 9. The figure shows that the models predict both

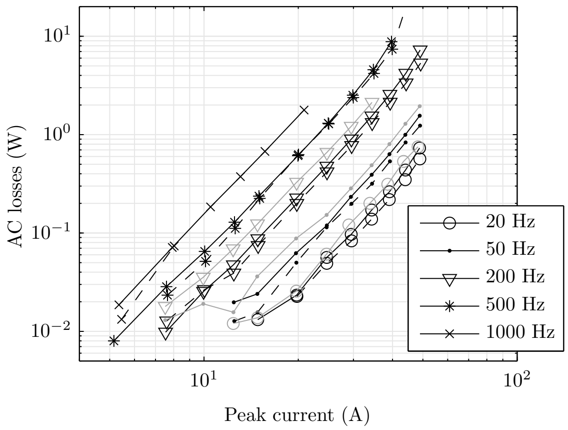

Fig. 8. Measured AC loss per cycle for sinusoidal (solid black lines), triangular (dashed black lines) and trapezoidal (solid gray lines) current waveforms, for different frequencies and peak values of the current.

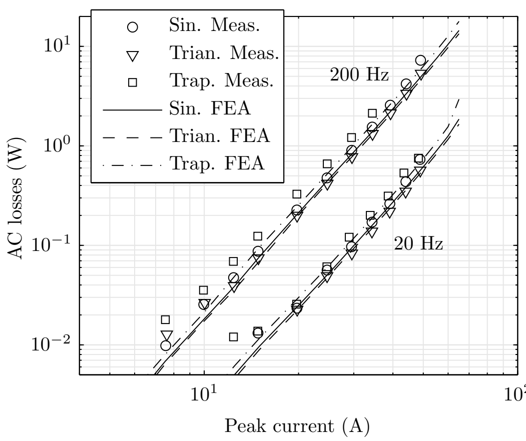

Fig. 9. AC losses for currents with a fundamental frequency of 20 Hz and 200 Hz, for measured and simulated losses with sinusoidal, triangular, and trapezoidal currents.

the absolute value of the AC losses, as well as the relative differences in the AC losses between the different waveforms.

The measured losses in case of sinusoidal, triangular and trapezoidal currents are compared to the modeled losses over their full range in Fig. 10. The models match well with the measurements for all waveforms for frequencies up to 200 Hz. However the models underestimate the measured losses at higher frequencies. While in the measurements the losses per cycle increase slightly with frequency, the losses per cycle in the models decreases at higher frequencies.

Table II shows the mean difference and the mean of the absolute value of the difference between the measured and simulated losses over the full range of amplitudes and frequencies for all waveforms. Additionally it shows the mean difference between the measured and modeled losses of the different waveforms compared to the sinusoidal waveform. On average, the models predict the measured losses with about 20% accuracy. The difference in the losses relative to those for sinusoidal currents are predicted by the models within 6 percentage points.

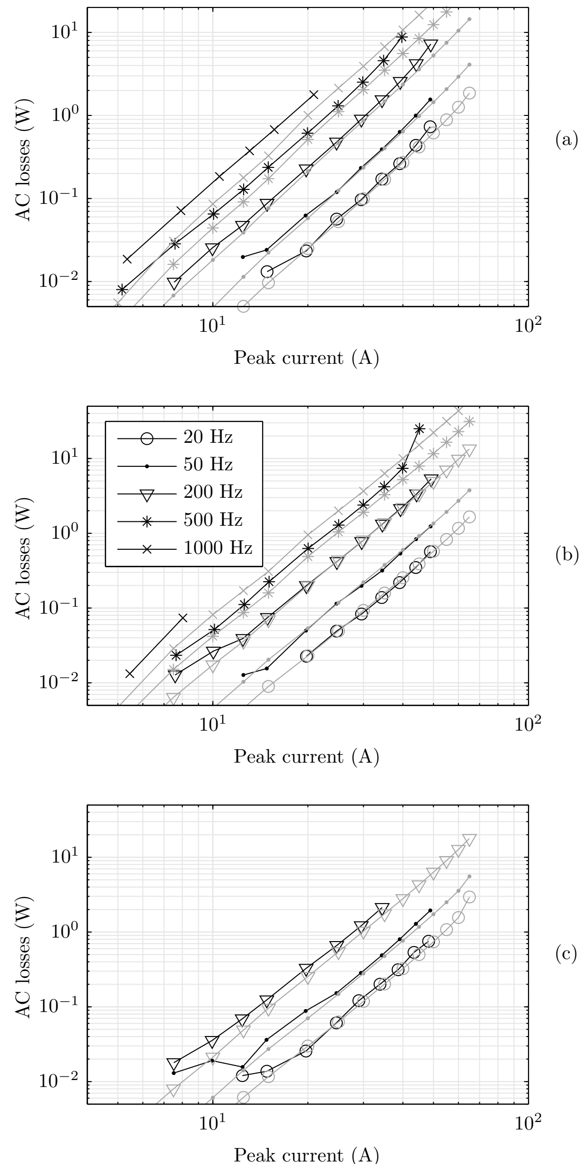

Fig. 10. Measured (black lines) and modeled (gray lines) AC losses as function of peak value of currents. For (a) sinusoidal currents, (b) triangular currents, and (c) trapezoidal currents.

TABLE II
MEAN AND ABSOLUTE DIFFERENCES BETWEEN MEASURED AND MODELED LOSSES.

	Sinusoidal	Triangular	Trapezoidal
mean(Meas.-Model)	+20%	+9%	+20%
mean(|Meas.-Model|)	21%	18%	22%
mean(Meas.-Meas. Sine)	0%	-13%	+16%
mean(Model-Model Sine)	0%	-7%	+17%

Lastly, losses with the current waveform equal to a dynamic motor application have been measured. The current waveform as shown in Fig. 4 was scaled to achieve waveforms with peak currents ranging from 5 A to 50 A. The AC losses obtained from measurements and simulation are shown in Fig. 11. For each value of peak current, measurement was repeated for 7

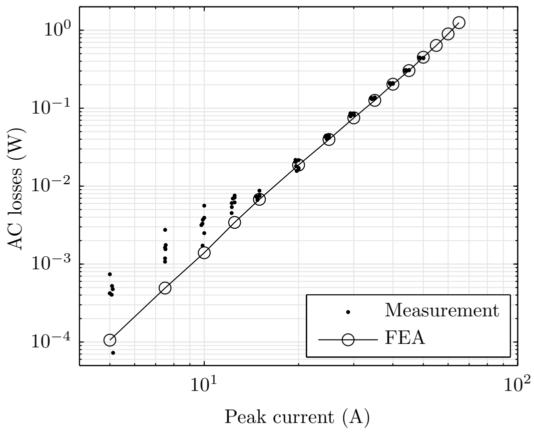

Fig. 11. AC losses as function of peak value for currents with the highly-dynamic profile shown in Fig. 4.

times. The maximum differences in measured and modeled losses are 0.3 mW for peak currents of 5 A, and 35 mW for peak currents of 50 A. For low values of the peak current, the measurements and models have discrepancy between 77% and 45%. However, for peak currents higher than 12.5 A (11% of the critical current of the tape), the difference between the measurement and model is lower than 7%. This makes the model suitable for the design of motor applications.

V. Discussion and conclusions

The proposed electrical measurement method is able to measure AC losses for non-sinusoidal current waveforms. The method is straightforward, and requires no calibration for the losses. However, the measurement instrument should be carefully designed not to introduce a phase shift between the measured voltage and current.

The finite element models including the power-law material description predict that the losses per cycle in the superconducting layer decrease towards higher frequencies. Additionally, as has been shown in this paper, they predicts different AC losses for different periodic signals with equal peak currents, unlike as is predicted by the critical state model. This mixed resistive and hysteretic behavior results from the exponential $E - J$ relation.

At frequencies below 100 Hz the losses as function of frequency in the measurements follow the trends predicted by the models. At higher frequencies, additional loss mechanisms become significant in the measurements. These are eddy current losses in the non-superconducting layers of the tapes and losses resulting from the slow thermal diffusion in the coil, which results in increased operating temperature of the superconducting tape.

The finite element models were able to predict the AC losses over a frequency range of 20 Hz to 1 kHz, for various current waveforms with an average difference to the measured values of 20%. Additionally, they are able to predict the dependency of the losses on the waveforms of the currents. A further investigation of additional loss mechanisms at high frequencies and losses is required.

Finally, it has been shown that losses can be measured and modeled for non-sinusoidal currents for dynamic motor applications using the modeling and measurement methods in this paper. For the demonstrated current waveform, losses can be estimated with an error lower than 7% for peak currents higher than 11% of the critical current. The validation of both the measurement and modeling methods opens the way for new superconducting power applications with superconducting tapes carrying non-sinusoidal and high-frequency currents.

References

[1] M. Zhang, M. Chudy, W. Wang, Y. Chen, Z. Huang, Z. Zhong, W. Yuan, J. Kvitkovic, S. V. Pamidi, and T. A. Coombs, "Ac loss estimation of hts armature windings for electric machines," *IEEE Transactions on Applied Superconductivity*, vol. 23, no. 3, pp. 5 900 604–5 900 604, June 2013.

[2] D. N. Nguyen, C. H. Kim, J. H. Kim, S. Pamidi, and S. P. Ashworth, "Electrical measurements of ac losses in high temperature superconducting coils at variable temperatures," *Superconductor Science and Technology*, vol. 26, no. 9, p. 095001, 2013.

[3] Z. Jiang, N. J. Long, M. Staines, R. A. Badcock, C. W. Bumby, R. G. Buckley, and N. Amemiya, "Ac loss measurements in hts coil assemblies with hybrid coil structures," *Superconductor Science and Technology*, vol. 29, no. 9, p. 095011, 2016.

[4] M. Zhang, W. Wang, Z. Huang, M. Baghdadi, W. Yuan, J. Kvitkovic, S. Pamidi, and T. Coombs, "Ac loss measurements for 2g hts racetrack coils with heat-shrink tube insulation," *Applied Superconductivity, IEEE Transactions on*, vol. 24, no. 3, pp. 1–4, June 2014.

[5] F. Grilli and S. P. Ashworth, "Quantifying ac losses in ybco coated conductor coils," *IEEE Transactions on Applied Superconductivity*, vol. 17, no. 2, pp. 3187–3190, June 2007.

[6] W. Yuan, T. A. Coombs, J.-H. Kim, C. H. Kim, J. Kvitkovic, and S. Pamidi, "Measurements and calculations of transport ac loss in second generation high temperature superconducting pancake coils," *Journal of Applied Physics*, vol. 110, no. 11, p. 113906, 2011.

[7] G. Li, H. Liu, Y. Wang, and H. Zhang, "Frequency-dependence and anisotropy of ac losses of bi2223/ag and ybco-coated conductors," *IEEE Transactions on Applied Superconductivity*, vol. 26, no. 4, pp. 1–4, June 2016.

[8] M. Tsuda, Y. Nakaide, D. Miyagi, and T. Hamajima, "Estimation method of ac losses in hts tape against a distorted current and/or a distorted magnetic field with harmonic components," *IEEE Transactions on Applied Superconductivity*, vol. 25, no. 3, pp. 1–5, June 2015.

[9] B. J. H. de Bruyn, J. W. Jansen, and E. A. Lomonova, "Comparison of force density of various superconducting linear motor types considering numerically evaluated ac losses," *IEEE Transactions on Applied Superconductivity*, vol. 26, no. 3, pp. 1–5, April 2016.

[10] T. Hardono, C. D. Cook, and J. X. Jin, "Calorimetric methods for measuring ac losses in htsc tapes carrying currents," *Superconductor Science and Technology*, vol. 11, no. 10, p. 1087, 1998.

[11] J. H. Kim, C. H. Kim, G. Iyyani, J. Kvitkovic, and S. Pamidi, "Transport ac loss measurements in superconducting coils," *IEEE Transactions on Applied Superconductivity*, vol. 21, no. 3, pp. 3269–3272, June 2011.

[12] H. Okamoto, F. Sumiyoshi, K. Miyoshi, and Y. Suzuki, "The nitrogen boil-off method for measuring ac losses in hts coils," *IEEE Transactions on Applied Superconductivity*, vol. 16, no. 2, pp. 105–107, June 2006.

[13] Y. Yang, E. Martnez, and W. T. Norris, "Configuration and calibration of pickup coils for measurement of ac loss in long superconductors," *Journal of Applied Physics*, vol. 96, no. 4, pp. 2141–2149, 2004.

[14] N. Amaro, J. ouc, J. Murta-Pina, J. Martins, J. M. Ceballos, and F. Gmry, "Contactless loop method for measurement of ac losses in hts coils," *IEEE Transactions on Applied Superconductivity*, vol. 25, no. 3, pp. 1–4, June 2015.

[15] N. Wimbush, Stuart; Strickland, "A high-temperature superconducting (hts) wire critical current database," https://doi.org/10.6084/m9.figshare.c.2861821.v3, accessed: Retrieved: 08 44, Feb 09, 2017 (GMT).

[16] R. Brambilla, F. Grilli, and L. Martini, "Development of an edge-element model for ac loss computation of high-temperature superconductors," *Superconductor Science and Technology*, vol. 20, no. 1, p. 16, 2007.

[17] "Comsol multiphysics user's guide," 2012.

[18] G. Mikitik, Y. Mawatari, A. Wan, and F. Sirois, “Analytical methods and formulas for modeling high temperature superconductors,” *Applied Superconductivity, IEEE Transactions on*, vol. 23, no. 2, pp. 8 001 920–8 001 920, April 2013.

[19] J. Rhyner, “Magnetic properties and ac-losses of superconductors with power law currentvoltage characteristics,” *Physica C: Superconductivity*, vol. 212, no. 3, pp. 292 – 300, 1993.

[20] I. D. Mayergoyz, “Nonlinear diffusion and superconducting hysteresis,” *IEEE Transactions on Magnetics*, vol. 32, no. 5, pp. 4192–4197, Sep 1996.

[21] F. Grilli, E. Pardo, A. Stenvall, D. Nguyen, W. Yuan, and F. Gomory, “Computation of losses in hts under the action of varying magnetic fields and currents,” *Applied Superconductivity, IEEE Transactions on*, vol. 24, no. 1, pp. 78–110, Feb 2014.

[22] Y. Zhao, C. Cheng, and C. Sorrell, “Frequency dependent behavior of ac loss in high temperature superconductors,” *Physica C: Superconductivity*, vol. 357360, Part 1, pp. 614 – 616, 2001.